

Investigation of Stress-Strain State of Ball Mill Trunnion



Ju. A. Bondarenko, S. I. Khanin and O. V. Bestuzheva

Abstract The article discusses the trunnion of a ball mill in the framework of the theory of elasticity, which is subjected to uneven thermal effects due to the heating load. Long-term operation of the mills leads to a significant wear of mainly mechanical parts of the supporting rotating parts—pins. There are various defects on the working surface of the trunnion, which, under the action of dynamic loads, contributes to the loss of working capacity and long downtime during repair. The study of the stress-strain state will determine the parameters for restoring the cylindrical surface of the trunnion. The equations describing the radial displacement of a point inside the trunnion of a ball mill are obtained. The equations describing the movement of the trunnion points of the ball mill are derived. The stress-strain state of the trunnion of the ball mill was determined depending on the temperature of the inner and outer surfaces of the trunnion. Deformations and stresses arising on the surface of a pin are investigated by numerical methods.

Keywords Ball mill · Trunnion · Stress-strain state

1 Introduction

In the production of building materials, main equipment for grinding raw materials is a ball mill. As a result of impact of free-falling grinding bodies, which are used as balls, grinding of raw materials takes place in a rotating drum along with material to be grounded under the action of centrifugal forces.

Long-term operation of the mills leads to a lot of wear and tear mainly to the mechanical parts supporting the rotating parts—trunnions. There are various defects

Ju. A. Bondarenko (✉) · S. I. Khanin
BSTU named after V.G. Shukhov, 46, Kostyukov Str., Belgorod 308012, Russia
e-mail: kdsm2002@mail.ru

O. V. Bestuzheva
Belgorod National Research University, 85, Pobedy Str., Belgorod 308015, Russia

© Springer Nature Switzerland AG 2020
A. A. Radionov et al. (eds.), *Proceedings of the 5th International Conference on Industrial Engineering (ICIE 2019)*, Lecture Notes in Mechanical Engineering,
https://doi.org/10.1007/978-3-030-22041-9_94

on the working surface of the trunnion. Dynamic loads contribute to the loss of efficiency and long downtime during repair. The study of the stress-strain state will determine the parameters for restoring the cylindrical surface of the trunnion.

2 Getting the Source Data for Mathematical Description of the Stress-Strain State of Trunnion

In the framework of the theory of elasticity, we consider a ball mill, which due to the heating of the loading materials, is subjected to an uneven thermal effect in terms of volume. As a result, there is a temperature field, which in turn, will lead to thermal deformations and stresses.

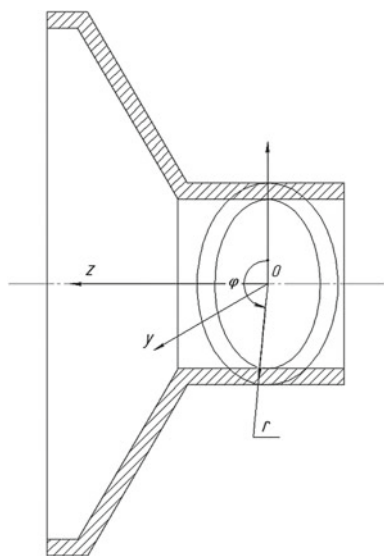
This section is devoted to the mathematical description of the deformation field and stresses in the ball mill axle. Among other reasons that cause stress-strain state of ball mill axle is the temperature field, which changes in the radial direction:

$$T = T(r), \quad (1)$$

where r varies in the following limits $R_1 \leq r \leq R_2$ (R_1 —inner radius of trunnion of ball mill; R_2 is the external radius of the axle).

In virtue of the axial symmetry, we introduce cylindrical coordinate system (r, φ, z) according to the design scheme presented in Fig. 1. The trunnion of ball mill will be considered as a thick-walled cylindrical tube with radial temperature change (1). Neglecting the influence of the ends can be assumed that in the perpendicular to the axis OZ of the sections are equal and are flat.

Fig. 1 Calculation scheme for choosing a coordinate system



On the basis of the made assumptions, we can conclude that the radial displacement of the point U in the trunnion of the ball mill depends only on one coordinate r , moving in the azimuthal direction, and elongation in the direction of OZ axis is constant:

$$\varepsilon_z = \text{const.} \quad (2)$$

In turn, relative elongations in radial direction:

$$\varepsilon_r = \frac{dU}{dr}, \quad (3)$$

in azimuthal direction:

$$\varepsilon_\phi = \frac{U}{r}. \quad (4)$$

The physical equations describing voltage field in cylindrical coordinates have following form [1]:

$$\sigma_z = 2G\varepsilon_z + \lambda\phi_0 - \eta T(r), \quad (5)$$

$$\sigma_r = 2G\varepsilon_r + \lambda\phi_0 - \eta T(r), \quad (6)$$

$$\sigma_\phi = 2G\varepsilon_\phi + \lambda\phi_0 - \eta T(r), \quad (7)$$

where $\sigma_z, \sigma_r, \sigma_\phi$ —respectively diagonal components of voltage tensor. For brevity, the following notation is entered as follows:

$$\phi_0 = \varepsilon_z + \lambda\varepsilon_r - \varepsilon_\phi, \quad (8)$$

$$\eta = 2G\alpha \frac{1+\nu}{1-2\nu}, \quad (9)$$

$$\lambda = \frac{2\nu G}{1-2\nu}, \quad (10)$$

$$G = \frac{E}{2(1+\nu)}. \quad (11)$$

where E —module of elasticity; ν —coefficient of Poisson; and α —coefficient of linear thermal expansion.

Substitutions (3), (4) in (6) and (7) allow to take next proportion:

$$\sigma_r = 2G \frac{dU}{dr} + \lambda\phi_0 - \eta T(r), \quad (12)$$

$$\sigma_\phi = 2G \frac{U}{r} + \lambda\phi_0 - \eta T(r), \quad (13)$$

Suppose that, as in the case of the solution of the thick-walled ring problem [2], the following equilibrium condition must be satisfied:

$$\sigma_r - \sigma_\phi r \frac{dU}{dr} = 0. \quad (14)$$

Expressions (2)–(14) are the starting point for obtaining the equations describing stress-strain state of trunnion of ball mill.

3 Getting the Source Data for Mathematical Description of the Stress-Strain State of Trunnion

According to the result of [2], if the inner and outer surfaces of the thick-walled pipe are maintained, respectively, constant temperature T_{R_1} and T_{R_2} , then for such a steady flow of temperature distribution over the wall thickness is the following formula:

$$T(r) = \frac{T_{R_1} \ln \frac{R_2}{r} + T_{R_2} \ln \frac{r}{R_1}}{\ln \frac{R_2}{R_1}}. \quad (15)$$

The motion of the point U is conveniently represented as an Integral with a variable upper limit:

$$U(r) = \frac{C_{10}}{r} + C_{20} \cdot r + \frac{\alpha}{r} \cdot \frac{1+\nu}{1-\nu} \int_{R_1}^r \chi T(x) dx. \quad (16)$$

To determine the arbitrary constants C_{10} and C_{20} , it is necessary to use the boundary conditions, which are superimposed on the stress values, acting on the inner R_1 and outer R_2 radiuses of the mill axle:

$$\sigma_r(r = R_1) = \sigma_0, \quad (17)$$

$$\sigma_r(r = R_2) = 0, \quad (18)$$

where σ_0 —the value of the voltage tested by the inner radius of the mill axle under the action of loading.

Substitution (15) in (16) and the application of boundary conditions and the condition of the absence of the axial load of the ball mill written as follows:

$$2\pi \int_{R_1}^{R_2} \sigma_z r dr = 0. \tag{19}$$

Allows to obtain unknown values C_{10} and C_{20} :

$$C_{10} = \frac{\alpha R_1^2(1 + \nu)}{4(1 - \nu)} \left[\frac{2(R_1^2 T_{R_1} - R_2^2 T_{R_2})}{R_2^2 - R_1^2} - \frac{T_{R_2} - T_{R_1}}{\ln\left(\frac{R_2}{R_1}\right)} \right], \tag{20}$$

$$C_{20} = \frac{\alpha}{2} \cdot \frac{(1 - 3\nu)}{(1 - \nu)} \left[\frac{R_2^2 T_{R_2} - R_1^2 T_{R_1}}{R_2^2 - R_1^2} - \frac{T_{R_1} - T_{R_2}}{2 \ln\left(\frac{R_2}{R_1}\right)} \right]. \tag{21}$$

The obtained Eqs. (20) and (21) allow to obtain a solution for (12)–(14):

$$\sigma_r = \frac{\alpha E}{2(1 - \nu)} \left[\frac{r^2 (R_2^2 T_{R_2} - R_1^2 T_{R_1}) + R_1^2 R_2^2 (T_{R_1} - T_{R_2})}{r^2 (R_2^2 - R_1^2)} - \frac{T_{R_1} \ln\left(\frac{R_2}{r}\right) + T_{R_2} \ln\left(\frac{r}{R_1}\right)}{\ln\left(\frac{R_2}{R_1}\right)} \right], \tag{22}$$

$$\begin{aligned} \sigma_\phi = & - \frac{\alpha E}{(1 - \nu)(R_2^2 - R_1^2) \ln\left(\frac{R_2}{R_1}\right)} \cdot \left\{ \left[\frac{R_1^2 R_2^2}{r^2} (T_{R_1} - T_{R_2}) + R_1^2 T_{R_1} - R_2^2 T_{R_2} \right] \ln\left(\frac{R_2}{R_1}\right) \right. \\ & \left. + (R_2^2 - R_1^2) \left(T_{R_2} \ln\left(\frac{r}{R_1}\right) + T_{R_1} \ln\left(\frac{R_2}{r}\right) \right) + T_{R_2} - T_{R_1} \right\}, \end{aligned} \tag{23}$$

and solution for (2)–(4):

$$\begin{aligned} \varepsilon_r = & \frac{\alpha}{2(1 - \nu)} \left[\frac{(1 - 3\nu)(R_2^2 T_{R_2} - R_1^2 T_{R_1})}{(R_2^2 - R_1^2)} + \frac{2\nu(T_{R_2} - T_{R_1}) + (1 + \nu) \left(T_{R_1} \ln\left(\frac{R_2}{r}\right) + T_{R_2} \ln\left(\frac{r}{R_1}\right) \right)}{\ln\left(\frac{R_2}{R_1}\right)} \right. \\ & \left. + \frac{(1 + \nu) R_1^2 R_2^2 (T_{R_1} - T_{R_2})}{r^2 (R_2^2 - R_1^2)} \right], \end{aligned} \tag{24}$$

$$\begin{aligned} \varepsilon_\phi = & \frac{\alpha}{2(1 - \nu)} \left[\frac{(1 - 3\nu)(R_2^2 T_{R_2} - R_1^2 T_{R_1})}{(R_2^2 - R_1^2)} - \frac{(1 - \nu)(T_{R_2} - T_{R_1}) - (1 + \nu) \left(T_{R_1} \ln\left(\frac{R_2}{r}\right) + T_{R_2} \ln\left(\frac{r}{R_1}\right) \right)}{\ln\left(\frac{R_2}{R_1}\right)} \right. \\ & \left. - \frac{(1 + \nu) R_1^2 R_2^2 (T_{R_1} - T_{R_2})}{r^2 (R_2^2 - R_1^2)} \right], \end{aligned} \tag{25}$$

$$\varepsilon_z = \frac{\alpha \left[(T_{R_2} - T_{R_1})(R_2^2 - R_1^2) + 2(R_1^2 T_{R_1} - R_2^2 T_{R_2}) \ln\left(\frac{R_2}{R_1}\right) \right]}{2(R_2^2 - R_1^2) \ln\left(\frac{R_2}{R_1}\right)} \quad (26)$$

The obtained ratios (22)–(26) determine the change in the stress-strain state of the ball mill axle depending on the temperature and the change in the radial distance from the axis of symmetry of the mill axle.

Based on the formulas (22, 23), find the stress values on the inner surface of the ball mill axle. To perform this operation, let $r = R_1$:

$$\sigma_z(r = R_1) = \sigma_\phi(r = R_1) = \frac{\alpha E(T_{R_2} - T_{R_1})}{1 - \nu} \left[\frac{R_2^2}{R_2^2 - R_1^2} - \frac{1}{2 \ln\left(\frac{R_2}{R_1}\right)} \right]. \quad (27)$$

When substituting $r = R_2$ in the ratio (22) and (23), we obtain the stress values for the outer surface of the ball mill axle:

$$\sigma_z(r = R_2) = \sigma_\phi(r = R_2) = \frac{\alpha E(T_{R_2} - T_{R_1})}{1 - \nu} \left[\frac{R_1^2}{R_2^2 - R_1^2} - \frac{1}{2 \ln\left(\frac{R_2}{R_1}\right)} \right]. \quad (28)$$

To find the deformation of the inner surface of the ball mill axle in the obtained ratios (24) and (25), substitute $r = R_1$:

$$\varepsilon_r(r = R_1) = \frac{\alpha}{1 - \nu} \left[\frac{T_{R_1}(R_2^2 - R_1^2) + \nu T_{R_1}(R_2^2 + R_1^2) - 2\nu T_{R_2} R_2^2}{R_2^2 - R_1^2} + \frac{\nu(T_{R_2} - T_{R_1})}{\ln\left(\frac{R_2}{R_1}\right)} \right], \quad (29)$$

$$\varepsilon_\phi(r = R_1) = \frac{\alpha}{2(1 - \nu)} \left[\frac{(1 - 3\nu)(R_2^2 T_{R_2} - R_1^2 T_{R_1}) + (1 + \nu)T_{R_1}(R_2^2 - R_1^2)}{R_2^2 - R_1^2} - \frac{(1 - \nu)(T_{R_2} - T_{R_1})}{\ln\left(\frac{R_2}{R_1}\right)} \right]. \quad (30)$$

To find deformations on the outer side of the ball mill axle in formulas (24) and (25), it is necessary to put $r = R_2$:

$$\varepsilon_r(r = R_2) = \frac{\alpha}{2(1 - \nu)} \left[\frac{(1 - 3\nu)(R_2^2 T_{R_2} - R_1^2 T_{R_1}) + (1 + \nu)T_{R_2}(R_2^2 - R_1^2)}{R_2^2 - R_1^2} + \frac{2\nu(T_{R_2} - T_{R_1})}{\ln\left(\frac{R_2}{R_1}\right)} \right], \quad (31)$$

$$\varepsilon_{\phi}(r = R_2) = \frac{\alpha}{2(1-\nu)} \left[\frac{(1-3\nu)(R_2^2 T_{R_2} - R_1^2 T_{R_1}) - (1+\nu)(R_1^2(T_{R_1} - T_{R_2}) + T_{R_2}(R_2^2 - R_1^2))}{R_2^2 - R_1^2} - \frac{(1-\nu)(T_{R_2} - T_{R_1})}{\ln\left(\frac{R_2}{R_1}\right)} \right]. \quad (32)$$

Thus, the obtained expressions (27)–(32) determine the stress-strain state of the inner and outer surface of the axle depending on the temperature inside and outside the ball mill axle.

4 Getting the Source Data for Mathematical Description of the Stress-Strain State of Trunnion

Under the action of the forces of the loading clinker, the potential energy of the inner part of the axle accumulates and in the process of moving the material into the housing turns into heat. When unloading, the thermal energy of the resulting cement from the housing also affects the inner surface of the unloading axle.

To derive the equations of dependence of the temperature of the inner surface along the length of the axle, it should be taken into account that the increase in the distance from the axle axis leads to a decrease in the heat flux density, which in this case is a variable. To calculate the heat loss through a cylindrical wall, the linear heat flux density is applicable:

$$q_l = \frac{Q}{l}. \quad (33)$$

According to the Fourier law, the amount of heat passing through the metal layer is equal to:

$$Q = -k_l \cdot F \frac{dt}{dr} = -\lambda \cdot 2\pi r \cdot l \frac{dt}{dr}. \quad (34)$$

When

$$q_l = -k_l \cdot 2\pi r \cdot \frac{dt}{dr}. \quad (35)$$

Substituting the boundary values of the variables and integrating the expression (34), according to [3], we obtain the following ratio:

$$\Delta t = -\frac{q_l}{2\pi k_l} \ln \frac{R_2}{R_1} + C. \quad (36)$$

Having determined the integration constant C [4], we obtain a calculation formula for determining the temperature change of the inner surface of the axle:

$$T_{R_1} = T_{R_2} - \frac{Q \ln \frac{R_2}{R_1}}{2\pi l k_l}, \quad (37)$$

where T_{R_1} —temperature of the inner surface of the axle, T_{R_2} —surface temperature of the axle, l —axle length, R_1 —inner radius of the trunnion of the ball mill, R_2 —external radius of the axle, and k_l —heat transfer coefficient calculated by the formula [5]:

$$k_l = \frac{1}{\frac{1}{\alpha_1 R_1} + \frac{1}{\lambda} \ln \frac{R_2}{R_1} + \frac{1}{\alpha_2 R_2}}, \quad (38)$$

where α_1 —heat transfer coefficient of the material to the inner surface of the axle, α_2 —heat transfer coefficient of the external surface of the axle to the air, and λ —thermal conductivity coefficient of steel.

The heat energy transferred from the inner to the outer surface of the axle will be equal to the amount of heat loaded from the clinker furnace during loading or cement during unloading [6]:

$$Q = q \cdot \rho \cdot V, \quad (39)$$

where q —specific heat of clinker/cement, ρ —density of the clinker when loading and when unloading cement, and V —volume of loaded and unloaded material.

Substituting all the initial values, the amount of heat during loading and unloading will be equal to [7]:

$$Q_{cl} = q_{cl} \cdot \rho_{cl} \cdot V = 0.88 \cdot 1400 \cdot 1.18 = 1454 \text{ J}, \quad (40)$$

$$Q_{cem} = q_{cem} \cdot \rho_{cem} \cdot V = 0.8 \cdot 1500 \cdot 1.18 = 1416 \text{ J}. \quad (41)$$

Since the magnitude of the heat amount of clinker only is slightly higher than the cement, take the value of the quantity of heat of clinker and look at the axle boot [8, 9].

Then, according to the found expressions (35)–(37), finding the temperature change of the inner surface of the axle along the length is made by the formula [10, 11]:

$$T_{R_1} = T_{R_2} - \frac{Q \cdot \ln \frac{R_2}{R_1}}{2\pi l k_l} = T_{R_2} - \frac{Q \cdot \ln \frac{R_2}{R_1}}{2\pi l \cdot \left(\frac{1}{\frac{1}{\alpha_1 R_1} + \frac{1}{\lambda} \ln \frac{R_2}{R_1} + \frac{1}{\alpha_2 R_2}} \right)}. \quad (41)$$

Consider the change in stresses and strains of the inner and outer surfaces of the axle along the length, substituting (40) depending on (29)–(32).

The change in the stresses of the inner and outer surface of the axle along the length is shown in Fig. 2. The internal surface stress along the longitudinal axis is

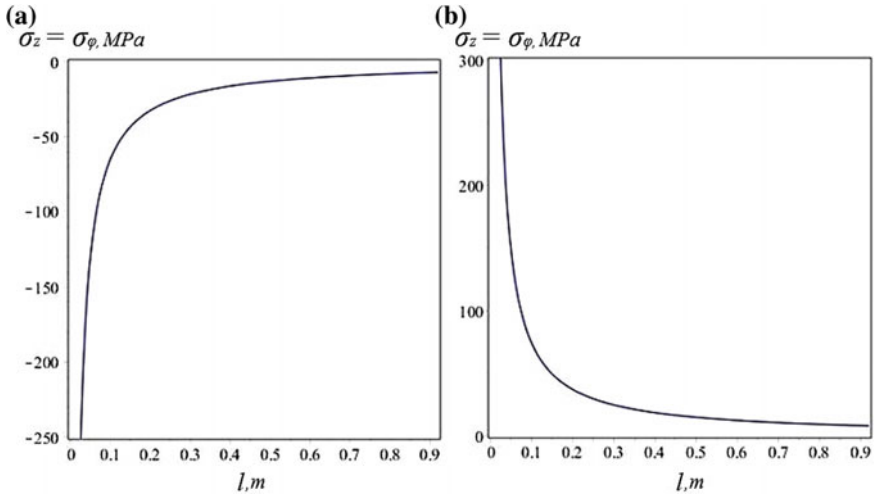


Fig. 2 The change in the voltage of the axle length **a** inner surface; **b** outer surface

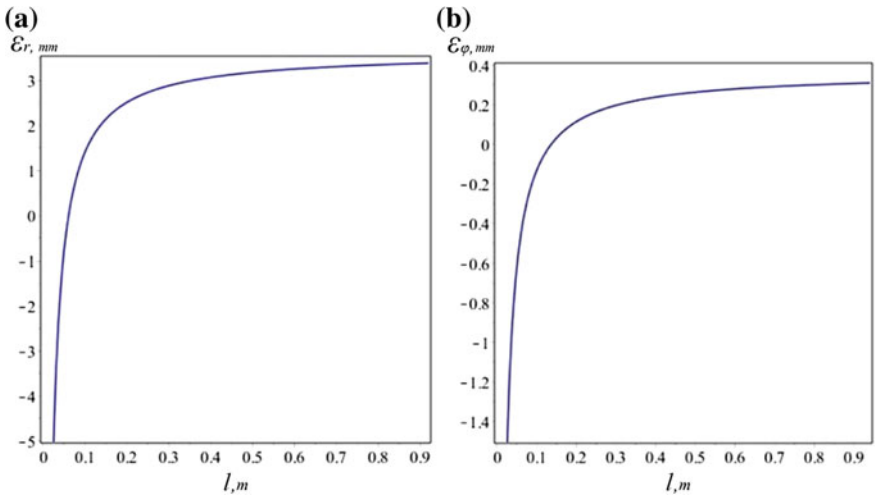


Fig. 3 Change of deformation of the inner surface of the axle along the length **a** in radial direction; **b** in azimuthal direction

only negative, indicating the influence of the internal surface temperature of the axle on the external surface of the axle [12, 13]. The change in the voltage of the outer surface along the length of the axle is characterized by an increase along the longitudinal axis from the bottom to the end [14, 15].

The change in deformations in both the radial and azimuthal direction of the inner surface of the axle along its length, shown in Fig. 3, shows the compression

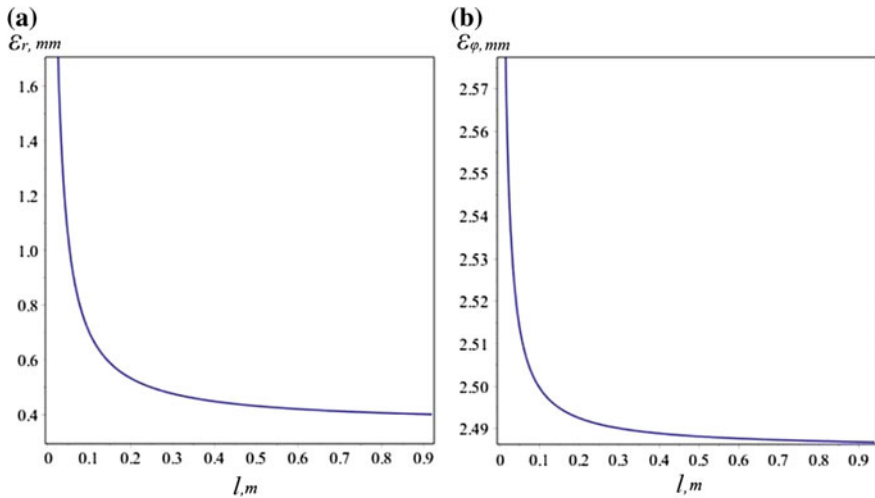


Fig. 4 Changing the deformation of the outer surface of the axle along the length **a** in radial direction; **b** in azimuthal direction

of the surface located closer to the bottom and the tension at the end of the axle [16, 17].

The deformation of the outer surface of the axle along the length in the radial and azimuthal directions is positive, which indicates tension (Fig. 4). In this case, when moving from the bottom to the end of the axle, the deformation of the outer surface decreases [18, 19]. The dependence of the deformation of the outer surface of the longitudinal coordinate is inverse [20].

Thus, the dependency graphs presented in Figs. 2, 3, and 4 characterize the stress-strain state along the length of the axle depending on the temperature of the inner surface.

References

1. Madera A (2005) Modeling of heat transfer in engineering systems. Moscow
2. Kartashov E, Kudinov V, Stefanyuk E (2012) Technical thermodynamics and heat transfer. Moscow
3. Timoshenko S, Gere J (2002) Mechanics of materials. Saint-Petersbourg
4. Bezukhov N (2011) Fundamentals of the theory of elasticity, plasticity and creep. Moscow
5. Birger I, Shorr B, Iosilevich G (2003) Calculation of the strength of machine parts. Moscow
6. Svetlickij V (2002) Mechanics of rods. Moscow
7. Filin A (2008) Applied mechanics of deformable solid. Moscow
8. Bogdanov O (2012) Handbook of ore dressing (in five volumes). Moscow
9. Pisarenko G, Mozharovskij N (2001) Equations and boundary value problems of the theory of elasticity and plasticity. Kiev

10. Bestuzheva O, Bondarenko J, Fedorenko M, Lipchanskaya J (2016) Machine for machining axles grinding mills. Russian Federation Patent 166615, 10 Dec 2016
11. Mukhachev V (2007) Planning and processing of experimental results. Tomsk
12. Rogov V, Poznyak G (2005) Methods and practice of technical experiments. Moscow
13. Daniel K (2009) The application of statistics to industrial experiments. Moscow
14. Afanasyeva N (2016) Computational and experimental methods of scientific experiment. Moscow
15. Research methods and organization of experiments (2013) Humanitarian center. Moscow
16. Bestuzheva O, Fedorenko M, Bondarenko J (2016) Experimental study of the recovery of a surface of revolution of large parts of industrial equipment. Bulletin of Belgorod State Technological University after V. G. Shukhov, vol 11, pp 122–127
17. Bestuzheva O, Fedorenko M, Bondarenko J (2016) Determination of the rational parameters of a rotating processing surfaces of rotation when restoring large parts. Bulletin of Belgorod State Technological University after V. G. Shukhov, vol 12, pp 121–125
18. Bestuzheva O, Fedorenko M, Bondarenko J, Sanina T (2016) Research of dependence of the area of the slice from the technological parameters and modes for the rotary machining of large parts. Technol Mech Eng 5:14–19
19. Bestuzheva O, Fedorenko M, Bondarenko J, Duganov Y (2016) Distortion of the cut surface of the workpiece in the form of a truncated cone with rotary processing. Technol Mech Eng 4:9–11
20. Sidnyaev N (2012) Theory of experiment planning and statistical data analysis. Moscow